

Singlet Excited-State Behavior of Uracil and Thymine in Aqueous Solution: A Combined Experimental and Computational Study of 11 Uracil Derivatives

Thomas Gustavsson,^{*,†} Ákos Bányász,^{†,‡} Elodie Lazzarotto,[†] Dimitra Markovitsi,[†] Giovanni Scalmani,[§] Michael J. Frisch,[§] Vincenzo Barone,^{||} and Roberto Improta^{*,||,∇}

Contribution from the Laboratoire Francis Perrin, CEA/DSM/DRECAM/SPAM - CNRS URA 2453, CEA Saclay, F-91191 Gif-sur-Yvette, France, Gaussian, Inc., 340 Quinipiac St. Bldg 40, Wallingford, Connecticut 06492, Dipartimento di Chimica, Università Federico II, Complesso Universitario Monte S. Angelo, Via Cintia, I-80126 Napoli, Italy, and Istituto Biostrutture e Bioimmagini/CNR, V. Mezzocannone 6-80134 Napoli, Italy

Received September 8, 2005; E-mail: thomas.gustavsson@cea.fr

Abstract: The excited-state properties of uracil, thymine, and nine other derivatives of uracil have been studied by steady-state and time-resolved spectroscopy. The excited-state lifetimes were measured using femtosecond fluorescence upconversion in the UV. The absorption and emission spectra of five representative compounds have been computed at the TD-DFT level, using the PBE0 exchange-correlation functional for ground- and excited-state geometry optimization and the Polarizable Continuum Model (PCM) to simulate the aqueous solution. The calculated spectra are in good agreement with the experimental ones. Experiments show that the excited-state lifetimes of all the compounds examined are dominated by an ultrafast (<100 fs) component. Only 5-substituted compounds show more complex behavior than uracil, exhibiting longer excited-state lifetimes and biexponential fluorescence decays. The S_0/S_1 conical intersection, located at CASSCF (8/8) level, is indeed characterized by pyramidalization and out of plane motion of the substituents on the C5 atom. A thorough analysis of the excited-state Potential Energy Surfaces, performed at the PCM/TD-DFT(PBE0) level in aqueous solution, shows that the energy barrier separating the local S_1 minimum from the conical intersection increases going from uracil through thymine to 5-fluorouracil, in agreement with the ordering of the experimental excited-state lifetime.

1. Introduction

Nucleic acids are known to undergo ultrafast internal conversion after photoexcitation in the UV-visible region.¹ This mechanism is supposed to have an enormous biological relevance by providing a natural limiting effect to photochemical damage due to UV absorption. However, despite numerous studies, the primary photoinduced processes in nucleic acids remain poorly understood.

As a first step toward a full understanding of the photoexcited processes occurring in the double helix, a large number of experimental and theoretical studies have thus been devoted to characterize the photophysical behavior of their building blocks (nucleobases, nucleosides, and nucleotides). All the bases absorb strongly in the UV region, and thus, a significant amount of energy is deposited in the absorbing excited state. However, such as in the case of nucleic acids, the nucleobases appear to be remarkably stable toward photodegradation, suggesting that

any possible photochemical processes are efficiently prevented by a fast nonradiative decay to the ground state.

Indeed, femtosecond time-resolved fluorescence and transient absorption studies agree in assigning subpicosecond lifetimes to the bright excited state of nucleobases in room-temperature aqueous solution, implying very efficient internal conversion processes.² In particular, fluorescence upconversion experiments³⁻⁷ on the monomeric DNA constituents have revealed that the fluorescence decays are extremely fast (<1 ps) and cannot be described by single exponentials, hinting at complex nonradiative deactivation processes occurring in the excited state(s).

In parallel to recent experimental work on the nucleobases, theoretical efforts have indeed begun to constitute an important source of valuable information, complementing the experimental studies in the characterization of the nature and the properties of the lowest electronically excited states and on the mechanism

[†] Laboratoire Francis Perrin.

[‡] Present address: Research Institute for Solid State Physics and Optics, Hungarian Academy of Sciences, P.O. Box 49, Budapest, Hungary H 1525.

[§] Gaussian, Inc.

^{||} Università Federico II.

[∇] Istituto Biostrutture e Bioimmagini.

(1) Bensasson, R. V.; Land, E. J.; Truscott, T. G. *Excited states and free radicals in Biology and Medicine*; Oxford University Press: Oxford, 1993.

(2) Crespo-Hernandez, C. E.; Cohen, B.; Hare, P. M.; Kohler, B. *Chem. Rev.* **2004**, *104*, 1977–2020.

(3) Peon, J.; Zewail, A. H. *Chem. Phys. Lett.* **2001**, *348*, 255–262.

(4) Gustavsson, T.; Sharonov, A.; Markovitsi, D. *Chem. Phys. Lett.* **2002**, *351*, 195–200.

(5) Gustavsson, T.; Sharonov, A.; Onidas, D.; Markovitsi, D. *Chem. Phys. Lett.* **2002**, *356*, 49–54.

(6) Onidas, D.; Markovitsi, D.; Marguet, S.; Sharonov, A.; Gustavsson, T. *J. Phys. Chem. B* **2002**, *106*, 11367–11374.

(7) Sharonov, A.; Gustavsson, T.; Carré, V.; Renault, E.; Markovitsi, D. *Chem. Phys. Lett.* **2003**, *380*, 173–180.

of their ultrafast decay.^{8–35} Unfortunately, while most of the available experimental results have been obtained in the condensed phase² (we refer here to room-temperature aqueous solution), the number of computational papers properly taking into account solvent effects is still limited.^{19,20,23–26,32} This makes the comparison between experiment and theory more difficult since the solvent is known to have a non-negligible effect on the excited-state properties of nucleobases. For example, in solution, the excited-state lifetimes do not exhibit the pronounced wavelength dependence that is found in gas-phase experiments.^{2,36,37} In this respect, it is worth noting that, even if extremely short excited-state lifetimes are observed also in the gas phase,^{38,39} there are several experimental results indicating that the excited-state lifetimes of uracil, thymine and adenine are shorter in room-temperature aqueous solution² than in the gas phase. Trapping for tens to hundreds of nanoseconds in a dark state has been reported to occur in the gas phase.^{40,41} Interestingly, in condensed phase at low temperatures, the luminescence lifetimes and quantum yields increase by several orders of magnitude.⁴²

In general, despite the enormous recent advances of time-resolved spectroscopic studies and theoretical efforts, the

underlying mechanism responsible for the excited-state decay of the different nucleobases is far from being fully assessed. What are the physicochemical factors (intramolecular as well as environmental) influencing the excited-state lifetime? Very likely, a general relaxation mechanism cannot be found that explains the ultrafast nonradiative deactivation of all monomers.

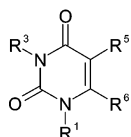
A very fruitful approach to shed light on the ground-state recovery mechanism has been to compare the excited-state behavior of different derivatives of the nucleobases. Already protonation/deprotonation may have a strong effect on the excited-state lifetime. Guanosine in acid solution (pH = 2–3) becomes protonated on the 7-position, which increases the lifetime from the subpicosecond range to about 200 ps.^{3,43,44} It is also well-known that substitution of the side groups may have a substantial influence on the excited-state properties, affecting the lifetime drastically. The most well-known example is 2-aminopurine, an adenine analogue with the amino group shifted from the 6- to the 2-position. For this reason, the excited-state lifetime increases by more than a factor of thousand from the picosecond to the nanosecond range.⁴⁵ Less drastic but still important effects have been observed for cytidine, where methylation on the 5-position increases the excited-state lifetime by a factor of 10.^{46,47} More generally, substitution (methylation) is a means to block specific reaction paths, such as proton/hydrogen transfer. An example is the study of adenine,⁴⁸ where the ambiguity induced by the presence of both 7H and 9H tautomers of adenine in aqueous solution was overcome by selected methylation.

We have used a similar strategy in this study, where the static and dynamical behaviors of the excited states of uracil and 10 of its derivatives have been characterized by means of femtosecond fluorescence upconversion and quantum chemical calculations.

Uracil and the closely related thymine (5-methyluracil) are the simplest nucleobases present in RNA and in DNA, respectively. They may therefore serve as “reference compounds” for a combined experimental and theoretical study. Furthermore, getting a closer insight on the excited-state features of the six-member pyrimidines could also help understanding the behavior of the purine bases (adenine and guanine). However, the number of accurate studies on uracil derivatives is still limited. Recently, a measure of the uracil excited-state lifetime using femtosecond transient absorption spectroscopy was reported.⁴⁹ The excited-state lifetime was found to be less than 200 fs, in principle, limited by the time resolution of the apparatus. From a computational point of view, even if the excited states of uracil have been studied at different levels of theory,^{24–26,28–32} to the best of our knowledge, there are only two studies devoted to the analysis of the excited-state deactivation mechanism,^{31,35} and they do not take into account solvent effects.

- (8) Ismail, N.; Blancafort, L.; Olivucci, M.; Kohler, B.; Robb, M. A. *J. Am. Chem. Soc.* **2002**, *124*, 6818–6819.
- (9) Merchán, M.; Serrano-Andrés, L. *J. Am. Chem. Soc.* **2003**, *125*, 8108–8109.
- (10) Blancafort, L.; Cohen, B.; Hare, P. M.; Kohler, B.; Robb, M. A. *J. Phys. Chem. A* **2005**, *109*, 4431–4436.
- (11) Perun, S.; Sobolewski, A. L.; Domcke, W. *Chem. Phys.* **2005**, *313*, 107–112.
- (12) Perun, S.; Sobolewski, A. L.; Domcke, W. *J. Am. Chem. Soc.* **2005**, *127*, 6257–6265.
- (13) Sobolewski, A. L.; Domcke, W.; Dedonder-Lardeux, C.; Jouvet, C. *Phys. Chem. Chem. Phys.* **2002**, *4*, 1093–1100.
- (14) Sobolewski, A. L.; Domcke, W. *Phys. Chem. Chem. Phys.* **2004**, *6*, 2763–2771.
- (15) Sobolewski, A. L.; Domcke, W. *Eur. Phys. J., D: Atom., Mol. Opt. Phys.* **2002**, *20*, 369–374.
- (16) Langer, H.; Doltsinis, N. L.; Marx, D. *ChemPhysChem* **2005**, *6*, 1734–1737.
- (17) Merchán, M.; Serrano-Andrés, L.; Robb, M. A.; Blancafort, L. *J. Am. Chem. Soc.* **2005**, *127*, 1820–1825.
- (18) Marian, C. M. *J. Chem. Phys.* **2005**, *122*, 104314.
- (19) Füllscher, M. P.; Serrano-Andrés, L.; Roos, B. O. *J. Am. Chem. Soc.* **1997**, *119*, 6168–6176.
- (20) Mennucci, B.; Toniolo, A.; Tomasi, J. J. *Phys. Chem. A* **2001**, *105*, 4749–4757.
- (21) Nielsen, S. B.; Sølling, T. I. *ChemPhysChem* **2005**, *6*, 1276–1281.
- (22) Chen, H.; Li, S. J. *Phys. Chem. A* **2005**, *109*, 8443–8446.
- (23) Broo, A.; Pearl, G.; Zerner, M. C. *J. Phys. Chem. A* **1997**, *101*, 2478–2488.
- (24) Marian, C. M.; Schneider, F.; Kleinschmidt, M.; Tatchen, J. *Eur. Phys. J., D: Atom., Mol. Opt. Phys.* **2002**, *20*, 357–367.
- (25) Shukla, M. K.; Leszczynski, J. *J. Phys. Chem. A* **2002**, *106*, 8642–8650.
- (26) Broo, A.; Holmén, A. J. *Phys. Chem. A* **1997**, *101*, 3589–3600.
- (27) Baraldi, I.; Bruni, M. C.; Costi, M. P.; Pecorari, P. *Photochem. Photobiol.* **1990**, *52*, 361–374.
- (28) Lorentzon, J.; Füllscher, M. P.; Roos, B. O. *J. Am. Chem. Soc.* **1995**, *117*, 9265–9273.
- (29) Shukla, M. K.; Mishra, P. C. *Chem. Phys.* **1999**, *240*, 319–329.
- (30) Neiss, C.; Saalfrank, P.; Parac, M.; Grimme, S. *J. Phys. Chem. A* **2003**, *107*, 140–147.
- (31) Matsika, S. *J. Phys. Chem. A* **2004**, *108*, 7584–7590.
- (32) Improta, R.; Barone, V. *J. Am. Chem. Soc.* **2004**, *126*, 14320–14321.
- (33) Tsolakidis, A.; Kaxiras, E. *J. Phys. Chem. A* **2005**, *109*, 2373–2380.
- (34) Matsika, S. *J. Phys. Chem. A* **2005**, *109*, 7538–7545.
- (35) Zgierski, M. Z.; Patchkovskii, S.; Fujiwara, T.; Lim, E. C. *J. Phys. Chem. A* **2005**, *109*, 9384–9387.
- (36) Ullrich, S.; Schultz, T.; Zgierski, M. Z.; Stolow, A. *J. Am. Chem. Soc.* **2004**, *126*, 2262–2263.
- (37) Ullrich, S.; Schultz, T.; Zgierski, M. Z.; Stolow, A. *Phys. Chem. Chem. Phys.* **2004**, *6*, 2796–2801.
- (38) Kang, H.; Lee, K. T.; Jung, B.; Ko, Y. J.; Kim, S. K. *J. Am. Chem. Soc.* **2002**, *124*, 12958–12959.
- (39) Canuel, C.; Mons, M.; Piuze, F.; Tardivel, B.; Dimicoli, I.; Elhanine, M. *J. Chem. Phys.* **2005**, *122*, 0743161–0743166.
- (40) He, Y.; Wu, C.; Kong, W. *J. Phys. Chem. A* **2003**, *107*, 5145–5148.
- (41) He, Y.; Wu, C.; Kong, W. *J. Phys. Chem. A* **2004**, *108*, 943–949.
- (42) Görner, H. *J. Photochem. Photobiol. B: Biol.* **1990**, *5*, 359–377.
- (43) Fujiwara, T.; Kamoshida, Y.; Morito, R.; Yamashita, M. *J. Photochem. Photobiol. B: Biol.* **1997**, *41*, 114–121.
- (44) Pecourt, J.-M. L.; Peon, J.; Kohler, B. *J. Am. Chem. Soc.* **2001**, *123*, 10370–10378.
- (45) Pal, S. K.; Peon, J.; Zewail, A. H. *Chem. Phys. Lett.* **2002**, *363*, 57–63.
- (46) Sharonov, A.; Gustavsson, T.; Marguet, S.; Markovitsi, D. *Photochem. Photobiol. Sci.* **2003**, *2*, 1–5.
- (47) Malone, R. J.; Miller, A. M.; Kohler, B. *Photochem. Photobiol.* **2003**, *77*, 158.
- (48) Cohen, B.; Hare, P. M.; Kohler, B. *J. Am. Chem. Soc.* **2003**, *125*, 13594–13601.
- (49) Cohen, B.; Crespo-Hernandez, C. E.; Kohler, B. *J. Chem. Soc., Faraday Discuss.* **2004**, *127*, 137–147.

Chart 1 Schematic Structure of the Substituted Uracils Studied in the Present Work, Where R¹, R², R³, and R⁴ Denote the Different Substituents Corresponding to the Table



	R ¹	R ²	R ³	R ⁴	R ⁵	R ⁶
U	H	H	H	H	H	H
1MU	Me	H	H	H	H	H
3MU	H	Me	H	H	H	H
T	H	H	Me	H	H	H
6MU	H	H	H	H	Me	H
1,3DMU	Me	Me	H	H	H	H
1MT	Me	H	Me	H	H	H
5FU	H	H	F	H	H	H
5CIU	H	H	Cl	H	H	H
TFT	H	H	CF ₃	H	H	H
5F1,3DMU	Me	Me	F	H	H	H

The 11 uracil derivatives treated in the present study (Chart 1) have been selected in order to cover substitution at different positions and of different chemical nature (electronegativity, weights, etc.), while multiple substitutions allowed us to verify the presence of additive and/or cooperative effects. Due to the fact that the theoretical characterization of excited states in solution recently has experienced very interesting advances, allowing accurate excited-state quantum chemical optimizations both in the gas phase^{8–31} and in solution (ref 32, and this will also be the subject of a forthcoming methodological article), the experimental results will be interpreted with the help of such calculations.

We have exploited these new possibilities in this joint experimental and computational study, that is aimed (i) to check how different substitutions in key position affect the excited-state behavior of uracil in aqueous solution; (ii) to accurately measure the effect of the ring substituent on the excited-state lifetime; (iii) to give an interpretation of the above results in terms of simple physicochemical effect; (iv) to understand what are the key mechanistic steps of the highly efficient nonradiative deactivation leading back to the ground state.

All the computational analysis hereby presented has been performed, including the effect of the aqueous solution environment. Besides its intrinsic interest, this study will thus hopefully constitute a critical test of the possibility of the recently developed quantum chemical methods to give a reliable picture of the excited-state process in the condensed phase.

2. Experimental Section

All compounds [uracil (U), 1-methyluracil (1MU), 3-methyluracil (3MU), thymine (5-methyluracil, T), 6-methyluracil (6MU), 1,3-dimethyluracil (1,3DMU), 1-methylthymine (1MT), 5-trifluoromethyluracil (trifluorothymine, TFT), 5-fluorouracil (5FU), 5-fluoro-1,3-dimethyluracil (5F1,3DMU), and 5-chlorouracil (5CIU); Chart 1] were purchased from Sigma Aldrich and used without further purification. They were dissolved in ultrapure water produced by a Millipore (Milli-Q Synthesis) purification system. Dihydrate quinine sulfate was obtained from Prolabo.

Absorption spectra were recorded with a Perkin Lamda 900 spectrophotometer using 1 mm, 2 mm, and 1 cm quartz cells (QZS). Fluorescence spectra were recorded with a SPEX Fluorolog-2 spectrofluorometer. The light source was a 450 W arc xenon lamp. Emission spectra were recorded with a band-pass of 4.71 nm at the excitation side and 2.25 nm at the emission side. The calibration of the emission monochromator was verified using an Hg low-pressure standard lamp, whereas that of the excitation monochromator was confirmed by observing the scattered excitation light from water. The emission correction factor was performed by means of deuterium and tungsten lamps of standard irradiance and checked via the standard fluorescence spectrum of quinine sulfate.⁵⁰

For the fluorescence measurements, 1 cm × 1 cm and 0.2 cm × 1 cm quartz cells (QZS) were used for dilute and concentrated solutions, respectively. For dilute solutions (<5 × 10⁻⁵ mol/dm⁻³), the water signal was not negligible compared to the fluorescence intensity. Therefore, its contribution was subtracted from the fluorescence spectra. In this way, the weak continuum was removed but the main Raman line could not be completely eliminated. To obtain the emission spectrum of a given solution over the whole near-UV and visible area, each spectrum was recorded twice: (i) without any filter at the emission side and using (ii) a Schott GG360 filter. The two spectra were normalized at an appropriate wavelength and then joined. Such a procedure allowed us to eliminate the second order of the scattered excitation light from water and Raman scattering (as well as the corresponding second-order features) so as to construct reliable fluorescence emission spectra over a large spectral domain.

Due to the relatively high concentration needed in order to get measurable fluorescence, reabsorption poses a problem. We overcame this by fitting the main part of the spectrum (where reabsorption can be neglected) with a log-normal function and then extrapolating toward shorter wavelengths. This treatment may also introduce a slight distortion in the blue wing, but we judge that this is of no consequence in the present work. Fluorescence quantum yields (ϕ_s) were determined using quinine sulfate dihydrate in 0.1 M HClO₄ ($\phi_s = 0.59$).⁵⁰ (For details of the quantum yield measurements, see Supporting Information.)

The femtosecond fluorescence upconversion setup has been described earlier.⁴ The excitation source is the third harmonic of a mode-locked Ti-sapphire laser. The 267 nm pulses are generated in a home-made frequency-tripler using two 0.5 mm type I BBO crystals. Typically, the average excitation power at 267 nm was 40 mW. The fluorescence from the sample is collected by parabolic mirrors and mixed with the residual fundamental in a 0.5 mm type I BBO crystal in order to generate the sum frequency. The sum frequency light is spectrally filtered in a small monochromator and detected by a photomultiplier in single-photon counting mode. The spectral resolution of the monochromator at the detection wavelength (223–288 nm) was set to 8 nm. Parallel ($I_{\text{par}}(t)$) and perpendicular ($I_{\text{perp}}(t)$) excitation/detection configurations were realized by controlling the polarization of the exciting beam with a zero-order half-wave plate.

Fluorescence decays were recorded at 330 nm. Temporal scans were made in a 4 ps time window with 33.3 fs steps in both parallel and perpendicular configurations.

The instrumental response function is well described by a Gaussian function $G(t)$, as confirmed separately by recording the fundamental Raman line of water at 295 nm. The full-width at half-maximum (fwhm) value of the Gaussian apparatus function is about 350 fs at 310 nm and decreases to below 300 fs at 450 nm, as expected from the GVD mismatch between the fluorescence and the fundamental in the sum frequency crystal. We judge that the time resolution of our setup is better than 100 fs after deconvolution, depending on the signal-to-noise ratio.

All measurements were performed at room temperature (20 ± 1 °C) under aerated conditions. Solutions (≈2.5 × 10⁻³ mol/dm⁻³) were kept flowing through a 0.4 mm quartz cell, which itself was kept in continuous motion perpendicular to the excitation beam. The power density cannot be measured precisely within the excitation volume, but we estimate it to be 0.2 ± 0.1 GW/cm² for a 40 mW output from the tripler unit.

Analysis. As shown in detail in the following section, both the absorption and the fluorescence spectra differ strongly in position and shape. As a consequence, to compare more easily and precisely the spectral properties of the different compounds examined, both absorption and fluorescence spectra were put on a frequency scale. Fluorescence spectra were scaled by a λ^2 factor and normalized. Subsequently,

(50) Velapoldi, R. A.; Mielenz, K. D. *A fluorescence standard reference material: quinine sulfate dihydrate*; U. S. Government Printing Office: Washington, D.C., 1980.

spectra were fitted with a simplified log-normal function⁵¹ to evaluate the extinction coefficient and the peak frequency. (For the actual form of the log-normal fitting function, see the Supporting Information.) Stokes shifts were calculated as the difference between the peak frequencies of the absorption and fluorescence spectra.

Fluorescence quantum yields were calculated using the relation

$$\phi_X = \frac{A_X (1 - 10^{-OD_S}) n_X^2}{A_S (1 - 10^{-OD_X}) n_S^2} \phi_S \quad (1)$$

where X refers to the studied compound and S to the reference compound quinine sulfate. (See Supporting Information for details.)

Total fluorescence kinetics $F(t)$ shown below were constructed from the parallel and perpendicular signals ($I_{\text{par}}(t)$ and $I_{\text{perp}}(t)$) according to the equation

$$F(t) = I_{\text{par}}(t) + 2I_{\text{perp}}(t) \quad (2)$$

Our recordings with parallel and perpendicular excitation/detection configuration allowed us to determine the fluorescence anisotropy $r(t)$. To this end, we performed a merged nonlinear fitting/deconvolution process using the impulse response model functions

$$i_{\text{par}}(t) = (1 + 2r(t))f(t) \quad (3)$$

$$i_{\text{perp}}(t) = (1 - r(t))f(t) \quad (4)$$

convoluted by the Gaussian instrument response function, $I(t) \propto i(t) \otimes G(t)$. The model functions thus obtained were fitted to the parallel (I_{par}) and perpendicular (I_{perp}) experimental signals. Mono- or biexponential functions were used for $f(t)$, while $r(t)$ was taken as monoexponential.

3. Computational Details

All of the calculations have been performed on the diketo form of uracil and its derivatives, which is the most stable form in the electronic ground state.^{24,52} It is by far the dominating tautomer both in gas phase^{53–56} and solution⁵⁷ even though the presence of the keto–enol tautomer has been reported, especially for 5-halogenated species.^{58,59} Moreover, the diketo is the only tautomer possible for all of the 1,3-dimethyl derivatives.

All of the calculations have been performed by using a development version of the Gaussian 03 package.⁶⁰ The absorption and emission spectra have been calculated by Time Dependent–Density Functional Theory (TD–DFT) using the PBE0 hybrid functional, which, despite the absence of adjustable parameters, has been shown to provide excitation spectra in very good agreement with experimental results and with an accuracy comparable to that of other hybrid functionals.^{32,61–64}

Three different basis sets were used, and geometry optimization was performed at the PBE0/6-31G(d) level⁶⁵ for S_0 and at the TD-PBE0/6-31G(d) level for S_1 . Analytical excited-state geometry optimizations have been performed at the PCM/TD-PBE0/6-31G(d) level in aqueous solution.⁶⁶ We verified that the Kohn–Sham orbitals mainly involved in the excitations are always very similar to the Hartree–Fock ones computed with the same basis set and are thus suitable for qualitative physical interpretation. We checked that all the computed frequency in the minima of the S_0 and S_1 surfaces are positive; for the S_0 surface, analytical second derivatives were used, while for S_1 , we performed numerical differentiation of analytic gradients.

Conical intersections (CI) between the ground and the π/π^* excited state have been located at the CASSCF(8/8)/6-31G(d) level, by using the method of Bearpark et al.,⁶⁷ including 6 π molecular orbital and the two n_O valence orbitals. The geometry of the CI is very similar to that obtained for uracil at the CASSCF(12/9) level,³¹ including all the 8 π orbitals and 1 n_O valence orbital. This latter structure has been shown to be reliable by single-point CASSCF calculation with larger expansion,³¹ suggesting that our approach should be fully adequate to the purposes of the present paper, namely, the comparison of the excited-state PES of different uracil derivatives. We therefore need just a good estimate of the CI structure to be used for the subsequent PCM/TD-PBE0 analysis of a wide region of the PES between the S_1 minimum and the CI.

Two-dimensional PESs have been computed at the PCM/TD-PBE0/6-31G(d) level in aqueous solution. The two coordinates are (i) the out of plane motion of the C5 substituent (ϕ , improper dihedral), (ii) a “collective” coordinate x , defined as a linear interpolation between the remaining internal coordinates of the minimum on S_1 and the CI. Such a reduction of the problem is justified by our computational results (see section 4.3.b. below).

Solvation Model. Bulk solvent effect on the UV spectra has been calculated by using the PCM/TD–DFT implementation described in refs 62 and 63. However, it is well-known that the proper description of solvent shifts in aqueous solutions requires the explicit inclusion of water molecules belonging to the first solvation shell in the cluster, which is further embedded in the dielectric continuum mimicking bulk solvent. Taking into account experimental suggestions,⁴¹ we thus include four explicit water molecules.³² The most stable arrangement (shown below) is in agreement with the indication of NMR experiments⁶⁸ that no water molecule is strongly bonded to C5 and C6 carbon atoms, and that O7 and O8 are coordinated by two and one water molecule, respectively. The results of a recent Car–Parrinello dynamics⁶⁹ suggest that the first coordination shell of uracil (up to 2.5 Å) is formed by 6 water molecules, 4 in the molecular plane (as in Figure 1) and 2 more or less perpendicular to it. Although a full description of the first solvation shell in solution requires, of course, a proper dynamic treatment, a number of studies have confirmed that the PCM is able to accurately account for the effect of water molecules that are more distant and/or not directionally bound to the carbonyl oxygen lone pairs.^{70,71}

4. Results

4.1. Steady-State Spectroscopy: Absorption. 4.1.a. Experimental Absorption Spectra. Steady-state absorption spectra of the uracils in room-temperature aqueous solution were analyzed as described above, and resulting spectral parameters

- (51) Siano, D. B.; Metzler, D. E. *J. Chem. Phys.* **1969**, *51*, 1856–1861.
 (52) Estrin, D. A.; Paglieri, L.; Corongiu, G. *J. Phys. Chem.* **1994**, *98*, 5653–5660.
 (53) Nowak, M. J.; Szczepaniak, K.; Barski, A.; Shugar, D. *Z. Naturforsch. C* **1978**, *33*, 876.
 (54) Brown, R. D.; Godfrey, P. D.; McNaughton, D.; Pierlot, A. P. *J. Am. Chem. Soc.* **1988**, *110*, 2329–2330.
 (55) Viant, M. R.; Fellers, R. S.; McLaughlin, R. P.; Saykally, R. J. *J. Chem. Phys.* **1995**, *103*, 9502–9505.
 (56) Colarusso, P.; Zhang, K.; Guo, B.; Bernath, P. F. *Chem. Phys. Lett.* **1997**, *269*, 39–48.
 (57) Becker, R. S.; Kogan, G. *Photochem. Photobiol.* **1980**, *31*, 5–13.
 (58) Morsy, M. A.; Al-Somali, A. M.; Suwaiyan, A. *J. Phys. Chem. B* **1999**, *103*, 11205–11210.
 (59) Markova, N.; Enchev, V.; Timtcheva, I. *J. Phys. Chem. A* **2005**, *109*, 1981–1988.
 (60) Frisch, M. J.; et al. In *Gaussian Development Version*, revision D.02; Gaussian, Inc.: Wallingford, CT, 2005.
 (61) Adamo, C.; Scuseria, G. E.; Barone, V. *J. Chem. Phys.* **1999**, *111*, 2889–2899.
 (62) Cossi, M.; Barone, V. *J. Phys. Chem. A* **2000**, *104*, 10614–10622.
 (63) Cossi, M.; Barone, V. *J. Chem. Phys.* **2001**, *115*, 4708–4717.
 (64) Improta, R.; Santoro, F.; Dieltl, C.; Papastathopoulos, E.; Gerber, G. *Chem. Phys. Lett.* **2004**, *387*, 509–516.

- (65) Adamo, C.; Barone, V. *J. Chem. Phys.* **1999**, *110*, 6158–6170.
 (66) Improta, R.; Barone, V.; Frisch, M. J.; Scalmani, G. In preparation.
 (67) Bearpark, M. J.; Robb, M. A.; Schlegel, H. B. *Chem. Phys. Lett.* **1994**, *223*, 269–274.
 (68) Chahinian, M.; Seba, H. B.; Ancian, B. *Chem. Phys. Lett.* **1998**, *285*, 337–345.
 (69) Gaigeot, M.-P.; Sprik, M. *J. Phys. Chem. B* **2004**, *108*, 7458–7467.
 (70) Improta, R.; Barone, V. *Chem. Rev.* **2004**, *104*, 1231–1254.
 (71) Adamo, C.; Cossi, M.; Rega, N.; Barone, V. In *Theoretical biochemistry. processes and properties of biological systems*; Eriksson, L., Ed.; Elsevier: Amsterdam, 2001; pp 467–538.

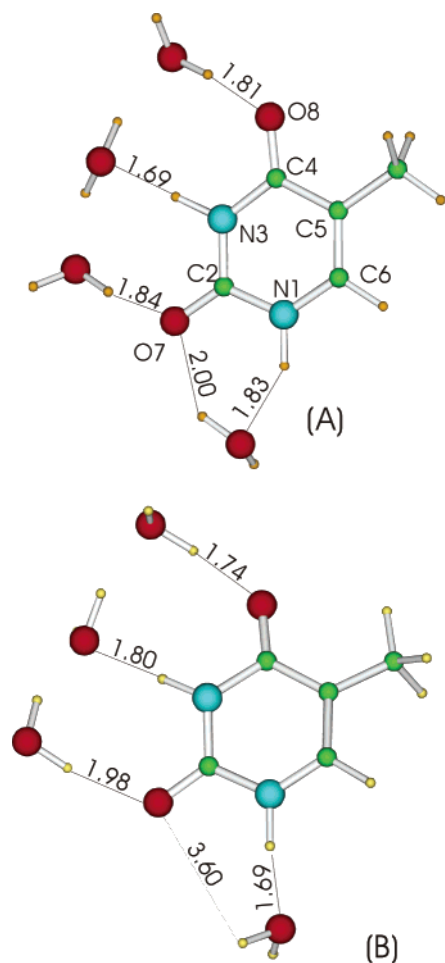


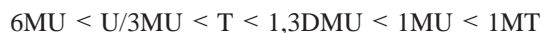
Figure 1. Schematic drawing of the minimum energy geometry of the ground (A) and first excited state (B) of the adduct formed by thymine and four water molecules.

as well as molar extinction coefficients are reported in Table 1. The absorption spectra of five chosen uracils (U), 6-methyluracil (6MU), 1,3-dimethyluracil (1,3DMU), thymine (T), and 5-fluorouracil (5FU), in aqueous solution are shown in Figure 2. (Absorption spectra of all uracils are given in the Supporting Information.)

The measured absorption maxima for uracil, thymine, 5-fluorouracil, and 5-chlorouracil compare well with the results present in the literature.^{72–78} The values we found for the molar extinction coefficients are, in most cases, slightly higher than those previously reported for uracil^{72–75} and thymine.^{72,73} This may be due to the hygroscopic character of the powders. One value given for thymine ($9.6 \times 10^3 \text{ M}^{-1}\text{cm}^{-1}$)⁷⁵ is surprisingly high.

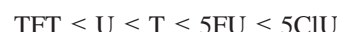
The comparison of the results obtained for the 11 studied compounds allows us to highlight some interesting features regarding their absorption spectra:

First, for what concerns methyl-substituted compounds, they are increasingly red-shifted in the order (on a wavelength scale)



Methyl substitution in positions 1 and 5 leads to a noticeable red shift of the absorption maxima. As a matter of fact, both thymine and 1-methyluracil peaks are ca. 1000 cm^{-1} red-shifted with respect to that of uracil. The effect of the methyl substituent in positions 1 and 5 seems to be additive, as shown by the maximum of 1-methylthymine, that is ca. 2000 cm^{-1} red-shifted with respect to uracil. On the other hand, methyl substituent in positions 3 and 6 does not lead to significant red shift of the absorption maxima. Actually, the 6-methyluracil peak is slightly blue-shifted with respect to the uracil one.

Moreover, absorption spectra of 5-substituted compounds are increasingly red-shifted in the order (on a wavelength scale)



This is in line with the findings of Lohmann who studied uracil and its 5-halogenated derivatives.⁷⁷

It may be worthwhile to note that the red shift introduced by the methyl substituents in the 1 and 3 positions seems to be additive with the spectral shift caused by the 5-fluoro substituent resulting in a ca. 2000 cm^{-1} red shift of 5F1,3DMU with respect to uracil.

4.1.b. Computed Absorption Spectra. To rationalize the results reported in the previous subsection and to check the reliability of our theoretical procedure, we computed the absorption spectra in aqueous solution of a representative subset of the examined compounds, namely, uracil, thymine, 5-fluorouracil, 6-methyluracil, and 1,3-dimethyluracil. As anticipated above, we took into account both bulk solvent effect by means of PCM method and cybotactic effects by studying the super molecule sketched in Figure 1, which includes four water molecules of the first solvation shell.

To better appreciate the importance of including solvent effect, the gas-phase results are also reported. In agreement with previous computational results, a strong absorption peak is predicted around $40\,000 \text{ cm}^{-1}$, arising from the HOMO–LUMO π/π^* transition.

The computed absorption maxima on the PCM level (Table 2) are in good agreement with the experimental ones, but for a small blue shift (ca. 2500 cm^{-1}), likely due to the overstabilization of the π bonding orbital by TD–DFT methods. On the other hand, it is encouraging that TD–DFT calculations correctly reproduce substituent effect on the transition energy. Taking uracil as reference compound, the transition is predicted to be blue-shifted in 6-methyluracil and red-shifted in 1,3-dimethyluracil, thymine, and 5-fluorouracil. The computed transition energies of 1,3-dimethyluracil and thymine are always similar, the energy difference being ca. 300 cm^{-1} and the relative energy ordering changing according to the basis set used. Actually, experiments show that the peaks are within 200 cm^{-1} .

The only noticeable quantitative discrepancy between our calculations and the experimental results is found for 5-fluorouracil, whose transition energy is similar to that of thymine and 1,3-dimethyluracil according to experiments, whereas it is ca. 500 cm^{-1} red-shifted according to our calculations. Apart from the computational difficulties in treating the subtle balance

(72) Voet, D.; Gratzer, W. B.; Cox, R. A.; Doty, P. *Biopolymers* **1963**, *1*, 193–208.

(73) Beaven, G. H.; Holiday, E. R.; Johnson, E. A. In *The nucleic acids. Chemistry and biology*; Chargaff, E., Davidson, J. N., Eds.; Academic Press: New York, 1955; Vol. 1.

(74) Clark, L. B.; Tinoco, I., Jr. *J. Am. Chem. Soc.* **1965**, *87*, 11–15.

(75) Kleinwachter, V.; Drobnik, J.; Augenstein, L. *Photochem. Photobiol.* **1966**, *5*, 579–586.

(76) Daniels, M.; Hauswirth, W. *Science* **1971**, *171*, 675–677.

(77) Lohmann, W. Z. *Naturforsch. C* **1974**, *29*, 493–495.

(78) Aaron, J. J.; Gaye, M. D. *Talanta* **1988**, *35*, 513–518.

Table 1. Characteristic Parameters of the First Absorption and Fluorescence Bands of Uracil and Its Derivatives: The Peak Molar Extinction Coefficient, ϵ_{\max} , the Peak Frequency, ν_{\max} , the Peak Wavelength, λ_{\max} , the Fluorescence Quantum Yield, Φ_F , and the Stokes Shift, $\Delta\nu$ (peak absorption minus peak fluorescence). Literature Data Are Shown in Italic

compound	Absorption			Fluorescence			
	ϵ_{\max} ($10^3 \text{ M}^{-1} \text{ cm}^{-1}$)	ν_{\max} (cm^{-1})	λ_{\max} (nm)	ν_{\max} (cm^{-1})	λ_{\max} (nm)	Φ_F ($\times 10^4$)	$\Delta\nu$ (cm^{-1})
U	9.1 8.2 ^{a,c} 8.1 ^b	38642	259 259.5 ^a 259 ^{b,c} 258.4 ^d 258 ^{e,f}	31301	312 308 ^e	0.35 0.45 ^e 1.16 ^k	7342
1MU	9.9	37400	267	31079	315	0.48	6320
3MU	7.4	38629	259	31578	311	0.38	7052
6MU	9.3	38861	257	31051	313	0.62	7809
T	8.4 7.9 ^a 9.6 ^c	37780	265 265 ^{e,f} 264.5 ^a 264 ^c	29934	329 ~330 ^{g,h,i}	1.02 ^e 1.75 ^k	7846
1,3DMU	9.6 8.9 ^c	37572	266 266 ^c	31513	312	0.47	6058
1MT	9.2	36720	272	29836	332	1.37	6884
5FU	6.1	37600	266 265.3 ^d	29447	335	2.21	8153
5CIU	7.9	36560	273 274.1 ^d 271 ^j	28557	345 340 ^j	0.91	8004
TFT	8.5	38918	257	31544	311	0.64	7375
5F1,3DMU	7.9	36572	273	28753	342	2.01	7820

^a From ref 72 (based on data from ref 73). ^b Reference 74. ^c Reference 75. ^d Reference 77. ^e Reference 76. ^f Reference 78. ^g Reference 79. ^h Reference 80. ⁱ Reference 81. ^j Reference 82. ^k Reference 83.

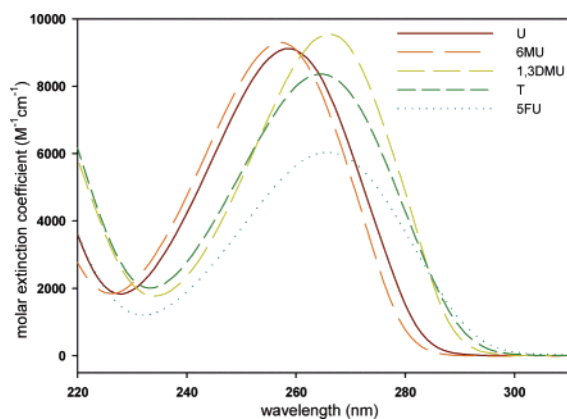


Figure 2. Steady-state absorption spectra of five uracils in room-temperature aqueous solutions: uracil (U), 6-methyluracil (6MU), 1,3-dimethyluracil (1,3DMU), thymine (T), and 5-fluorouracil (5FU).

of hyperconjugative and electron-withdrawing effects associated with the fluoro substituent, it could be hypothesized that the first solvation shell should explicitly include a water molecule directly bound to the fluorine atom since C–F bonds are known to be frequently involved in nonconventional hydrogen bonding.^{84–86}

The analysis of the shape of the molecular orbitals involved in the electronic transition (Figure 3) allows us to rationalize the energy trends of the π/π^* transition. The methyl groups in

C5 and N1 and the fluoro substituent in C5 position give an antibonding contribution to the HOMO, thus increasing the HOMO energy. Their contributions are slightly antibonding also for the LUMO, but the weight of C5 and N1 (and their substituents) atomic orbitals is much larger in the HOMO with respect to the LUMO. When substituents able to give rise to a hyperconjugative effect are present in C5 or in N1, the HOMO–LUMO energy gap decreases and the S_0 – S_1 transition is red-shifted with respect to uracil.

Obviously, the interaction between the frontier orbitals depends also on the electronegativity of the C5 substituent. The strongly electron-withdrawing trifluoromethyl group has a bonding interaction with the molecular orbitals of the pyrimidine ring, which is more relevant for the HOMO. Our calculations, in agreement with the experimental results, predict that the π/π^* transition is ca. 500 cm^{-1} blue-shifted with respect to uracil (Table 2).

Similar considerations can also explain the different behavior of C6 substituents. In this case, the antibonding character of the C6–methyl interaction in the LUMO is larger than that of the HOMO, accounting for the weak blue shift. Finally, the contribution of N3 to the frontier orbitals of uracil derivatives is very small, explaining why substituents in that position do not lead to significant shift of the S_0 – S_1 electronic transition.

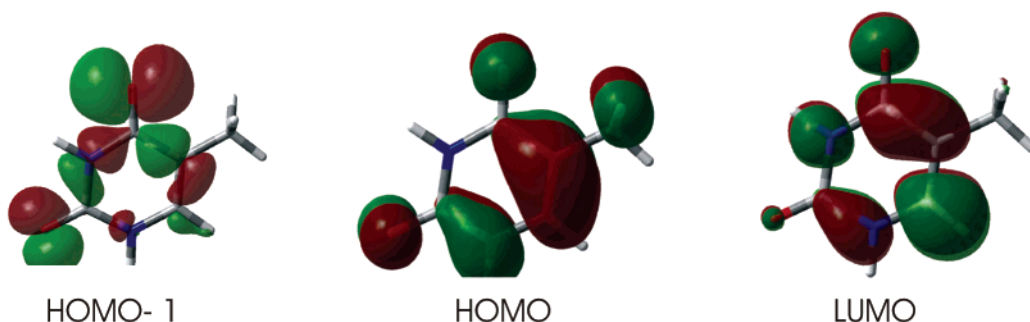
The inclusion of four water molecules of the first solvation shell does not significantly affect the relative transition energy of the five compounds examined, but slightly reduces the quantitative discrepancy between computed and experimental energy maxima. Actually, the π/π^* transitions are expected to be less affected by explicit hydrogen bonds than the n/π^* transitions, involving carbonyl lone pairs, that are instead significantly blue-shifted. On the other hand, a lot of caution has to be used when comparing the results relative to the systems including the first solvation shell. It could indeed be possible

- (79) Vigny, P.; Duquesne, M. *Photochem. Photobiol.* **1974**, *20*, 15–25.
 (80) Callis, P. R. *Chem. Phys. Lett.* **1979**, *61*, 563–567.
 (81) Callis, P. R. *Annu. Rev. Phys. Chem.* **1983**, *34*, 329–357.
 (82) Suwaiyan, A.; Morsy, M. A.; Odah, K. A. *Chem. Phys. Lett.* **1995**, *237*, 349–355.
 (83) Hauswirth, W.; Daniels, M. *Chem. Phys. Lett.* **1971**, *10*, 140–142.
 (84) Parsch, J.; Engels, J. W. *J. Am. Chem. Soc.* **2002**, *124*, 5664–5672.
 (85) van der Veken, B. J.; Herrebout, W. A.; Szostak, R.; Shchepkin, D. N.; Havlas, Z.; Hobza, P. *J. Am. Chem. Soc.* **2001**, *123*, 12290–12293.
 (86) Zierkiewicz, W.; Michalska, D.; Havlas, Z.; Hobza, P. *ChemPhysChem* **2002**, *3*, 511.

Table 2. Absorption Energy (in cm^{-1}) of the Two Lowest Energy Electronic Transitions in Five Uracil Derivatives. PBE0/6-31G(d) Geometry Optimizations in Aqueous Solution. A Dimensionless Oscillator Strength Is Given in Parentheses

	Gas Phase	Water solution PCM			Water solution PCM + 4H ₂ O		
	6-311 + G(2d,2p)	6-31G(d)	6-31 + G(d,p)	6-311 + G(2d,2p)	6-31G(d)	6-31 + G(d,p)	6-311 + G(2d,2p)
				uracil			
π/π^*	42423 (0.142)	43182 (0.179)	42215 (0.211)	41657 (0.198)	42937 (0.189)	42031 (0.212)	41489 (0.199)
n/π^*	38745	41116	41828	41586	42329	42760	42509
				thymine			
π/π^*	40836 (0.147)	42063 (0.183)	40783 (0.210)	40217 (0.200)	41869 (0.193)	40677 (0.210)	40122 (0.199)
n/π^*	39290	41384	41846	41609	42610	42807	42564
				5-fluorouracil			
π/π^*	40302 (0.133)	41211 (0.173)	40324 (0.197)	39737 (0.183)	40807 (0.186)	39987 (0.203)	39415 (0.190)
n/π^*	39094	41541	42073	41853	42609	42935	42705
				6-methyluracil			
π/π^*	42167 (0.168)	43014 (0.207)	42217 (0.244)	41726 (0.231)	42480 (0.150)	41823 (0.244)	41353 (0.238)
n/π^*	38294	41152	42067	41859	42615	43201	42966
				1,3-dimethyluracil			
π/π^*	41019 (0.156)	42003 (0.193)	41117 (0.221)	40568 (0.208)	41692 ^b (0.205)	40974 ^b (0.226)	40449 ^b (0.217)
n/π^*	39263	41327	41924	41659	43412	43776	43384

^a Trifluorothymine, PCM/TD-PBE0/6-311+G(2d,2p)//PBE0/6-31G(d) calculations in aqueous solution: $\pi/\pi^* = 42149(0.189)$. ^b Calculations with two explicit water molecules: 41951(0.195)/41121 (0.219)/40586(0.208).

**Figure 3.** Molecular orbitals involved in the HOMO–LUMO (π/π^*) and HOMO-1/LUMO (n/π^*) electronic transitions.

that the number of solvent molecules that should be explicitly considered is not the same for all the compounds examined, and that might affect the relative transition energy. It is, for example, significant that, when only two water molecules are included in the calculations, the transition energy of 1,3-dimethyluracil is blue-shifted by ca. 200 cm^{-1} , giving an estimate of the energy variation associated with different models of the cybotactic region. Shortly, while the inclusion of explicit water molecules increases the general reliability of our calculations, it may also introduce another (though small) possible source of error. For consistency, we choose to compare always the results with the same number of molecules.

Before analyzing the fluorescence spectra, it is important to highlight that for all the compounds examined π/π^* transition corresponds to the lowest energy one. The S_0-S_2 transition, corresponding to a dark n/π^* state, is quite close in energy, and for uracil, only when both bulk solvent effects and the cybotactic region are included in the calculation, the π/π^* transition becomes the lowest in energy.³² Interestingly, for all the compounds examined, the n/π^* transition would be the lowest in energy in the gas phase, confirming that any reliable computational analysis of the excited state behavior in condensed phase requires that solvent effects are properly taken into account.

In summary, in this section, we have shown that the absorption spectra of uracil derivatives critically depend on the nature and the position of the ring substituents, and that the energy trend can be convincingly explained by analyzing the shape of the molecular orbitals involved in the electronic transition. Furthermore, TD-PBE0 calculations satisfactorily reproduce substituent effect, while solvent effect can be effectively described using a hybrid model that includes explicitly the first solvation shell, while bulk effects are treated by the PCM method.

Finally, contrary to what was found in the gas phase,³¹ our calculations predict that in aqueous solution the lowest energy transition corresponds to the π/π^* transition. In the subsequent steps of our study, we will focus our attention mainly on this electronic state.

4.2. Steady-State Spectroscopy: Fluorescence. 4.2.a. Experimental Fluorescence Spectra. Steady-state fluorescence spectra of the uracils in room-temperature aqueous solution obtained for excitation at 255 nm were analyzed as described above, and resulting spectral parameters are reported in Table 1. Also given in Table 1 is the Stokes shift, that is, the difference in wavenumber between the absorption and the fluorescence maxima. The fluorescence spectra of five chosen uracils (U), 6-methyluracil (6MU), 1,3-dimethyluracil (1,3DMU), thymine

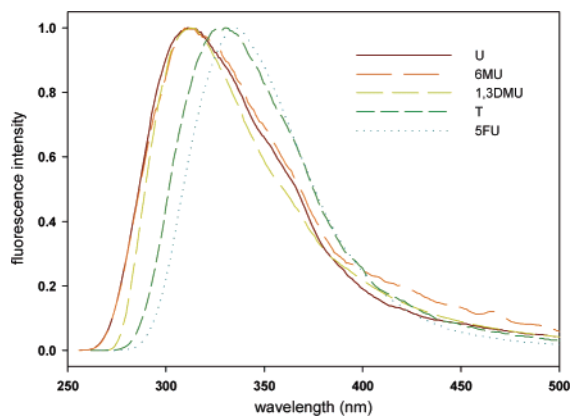


Figure 4. Steady-state fluorescence spectra of five uracils in room-temperature aqueous solutions: uracil (U), 6-methyluracil (6MU), 1,3-dimethyluracil (1,3DMU), thymine (T), and 5-fluorouracil (5FU).

(T), and 5-fluorouracil (5FU), in aqueous solution are shown in Figure 4. (Fluorescence spectra of all uracils are given in the Supporting Information.)

Fluorescence peak maxima have been reported for room-temperature aqueous solutions of uracil,⁷⁶ thymine,^{79–81} and 5-chlorouracil.⁸² Our values, 312, 329, and 345 nm, compare relatively well to literature values (Table 1).

In agreement with the results of previous studies, all the compounds examined exhibit a very large Stokes shift (~ 1 eV, $\sim 8 \times 10^3$ cm^{-1}), suggesting significant changes of the excited-state geometry. Actually, since the emission maxima do not follow the same trend as the absorption maxima, the Stokes shifts vary a lot, ranging from about 6000 cm^{-1} for 1,3-dimethyluracil to more than 8100 cm^{-1} for 5-fluorouracil.

For what concerns methyl-substituted uracil derivatives, the emission peaks are increasingly red-shifted in the order (on a wavelength scale)

$$3\text{MU} < \text{U}/1,3\text{DMU} < 6\text{MU} < 1\text{MU} < \text{T} < 1\text{MT}$$

Two subsets can be recognized in the above compounds. Although they were separated by more than 1000 cm^{-1} in absorption, the peaks of the compounds bearing a 5-methyl substituent (1MT and thymine) are very close and more than 1000 cm^{-1} red-shifted with respect to the remaining five. Those latter exhibit emission peaks very close (within 500 cm^{-1}), while the absorption maxima were dispersed in a range of ca. 1500 cm^{-1} .

The emission peaks of 5-substituted derivatives of uracil are increasingly red-shifted in the order (on a wavelength scale)

$$\text{TFT} < \text{U} < \text{T} < 5\text{FU} < 5\text{CIU}$$

This is the same trend as for the absorption peaks. However, also in this class of compounds, the Stokes shift is not uniform, being larger for 5-halo-substituted compounds and much smaller (ca. 800 cm^{-1}) for uracil and trifluorothymine. From a phenomenological point of view, the strong correlation of absorption and fluorescence spectra suggests that the 5-substituent affects ground-state and relaxed excited-state electronic structures in a similar (but not identical) manner.

4.2.b. Fluorescence Quantum Yields and Radiative Lifetimes. Fluorescence quantum yields for the 11 uracil derivatives are given in Table 1. One may note that there is a difference of nearly 1 order of magnitude between uracil and 5-fluorouracil.

Fluorescence quantum yields for uracil and thymine have been reported in ref 76 for excitation at the absorption maximum and in ref 83 for excitation at the 0–0 transition. Interestingly, the yield increases notably in the latter case. Our values compare well with the values given in ref 76.

No general correlation between the fluorescence quantum yields and any other observable can be established. It seems though that, for the 5-substituted uracil derivatives, the quantum yields are inversely proportional to the molar extinction coefficient, which is surprising and may indicate a significant change in electronic structure between the absorbing and the emitting states and/or a change of the nonradiative rate with substitution. For the methylated uracil derivatives, the quantum yields are inversely proportional to fluorescence peak values, which likewise may indicate a change of the nonradiative rate with the position of substitution.

Radiative lifetimes were calculated from steady-state absorption and fluorescence spectra using the Strickler–Berg relation.⁸⁷ Combining these values with the measured fluorescence quantum yields, approximate fluorescence lifetimes could be calculated using the relation

$$\tau_{\text{F}} = \tau_{\text{rad}} \times \Phi_{\text{F}} \quad (5)$$

Resulting values are reported in Table 4. One may note that all the radiative lifetimes are relatively short, ranging between 7 and 10 ns, which corresponds to allowed transitions. The radiative lifetimes follow closely the inverse of the molar extinction coefficients, which results from the Strickler–Berg treatment. The estimated fluorescence lifetimes are of course much faster, due to the very small quantum yields. The spread is larger than that for the radiative lifetimes, ranging from 0.25 to 2.2 ps, which basically follow the trend of the fluorescence quantum yields.

4.2.c. Computed Fluorescence Spectra. In the next step of our theoretical analysis, we have optimized the geometry in aqueous solution at the PCM/TD-PBE0/6-31G(d) level corresponding to the minima of the first excited state (Table 3). We found stable local energy minima in the proximity of the Franck–Condon (FC) point for all the compounds, except for 6-methyluracil. For this compound, excited-state geometry optimization leads directly toward a region of the PES where the S_0 and S_1 state are close to be isoenergetic (i.e., close to the S_0/S_1 conical intersection; see below). TD–DFT geometry optimizations predict significant distortion from planarity of the pyrimidine ring that assumes a “boat-like” conformation, with N3 and C6 out of the plane defined by N1, C2, C4, and C5 that are indeed close to being coplanar (Figure 5).

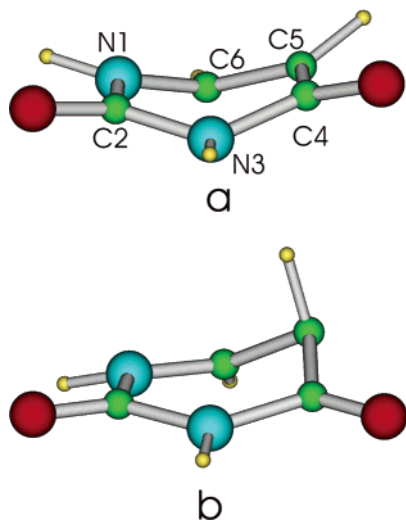
While N3 is significantly pyramidalized in all of the compounds, in thymine and 5-fluorouracil, the geometry around C6 is still close to being planar (H–C6–N1–C5 improper dihedral angles being 172 and 176°, respectively). The geometry of the carbonyl moieties is also very close to planarity. Not surprisingly, the largest variations of the bond lengths involve the lengthening of C5–C6, C4–O8, and N3–C4 bond distances and the shortening of C4–C5 bond distance, in line with the bonding/antibonding character of HOMO and LUMO with respect to those bonds (Figure 3).

(87) Strickler, S. J.; Berg, R. A. *J. Chem. Phys.* **1962**, *37*, 814–822.

Table 3. Fluorescence Energy (in cm^{-1}) of the Lowest Energy Electronic Transition in Five Uracil Derivatives. PBE0/6-31G(d) Geometry Optimizations in Aqueous Solution. Dimensionless Oscillator Strengths Are Given in Parentheses

	PCM			PCM+4H ₂ O		
	6-31G(d)	6-31+G (d,p)	6-311+G (2d,2p)	6-31G(d)	6-31+G (d,p)	6-311+G (2d,2p)
U	28830 (0.20)	28034 (0.23)	27745 (0.22)	31357 (0.23)	30574 (0.26)	30255 (0.25)
T	29238 (0.21)	28309 (0.24)	27969 (0.23)	31566 (0.25)	30584 (0.27)	30206 (0.26)
5FU	29518 (0.20)	28812 (0.23)	28482 (0.22)	31105 (0.23)	30452 (0.25)	30097 (0.24)
6MU	<i>a</i>	<i>a</i>	<i>a</i>	<i>a</i>	<i>a</i>	<i>a</i>
13DMU	27978 (0.20)	27270 (0.22)	27013 (0.22)	29122 (0.22)	28540 (0.23)	28230 (0.22)

^a Goes directly toward the CI.

**Figure 5.** Geometry of uracil (a) in the minimum of π/π^* electronic state (b) in the S_1/S_0 conical intersection.

The significant geometry distortion upon electron excitation is in line with the diffuseness of the jet-cooled absorption spectra,⁸⁸ and the computed geometry shifts are similar to that obtained at the DFT/MRCI level²⁴ in the gas phase.

When only bulk solvent effects are included, the computed fluorescence energies are much lower than the experimental maxima, suggesting that some important effect has not been taken properly into account by our calculations. Since our previous study on uracil excited state shows that the coordination geometry of the first solvation shell remarkably depends on the electronic state of the solute,³² we have optimized the excited-state geometry including four explicit water molecules (Figure 1b). The coordination geometry of the water molecules in the excited state is actually quite different from that predicted for the ground state. The computed fluorescence energy is then much closer to the experimental one, and the relative energy ordering is similar to that predicted by experiments (with the exception of 1,3-dimethyluracil), supporting the reliability of the excited-state geometry minima we determined.

On the other hand, despite the improvement observed after the inclusion of the explicit water molecules, the energy difference among the emission peaks of the five compounds examined is not very close to the experimental one. Also, the emission energy of 1,3-dimethyluracil is predicted to be the lowest among the compounds examined, in disagreement with

the experimental results. This can be, at least partially, due to the different specific solvation effect (the presence of methyl substituents on the nitrogen atom could significantly alter the first solvation shell). When only bulk effects are considered, the disagreement with the experiments for what concerns the relative energy difference with respect to uracil is significantly reduced.

However, before comparing experimental and computational results, it is important to remember that a lot of caution has to be used when analyzing the fluorescence peak values for the compounds with ultrashort fluorescence lifetimes. Steady-state spectra may be dominated by fluorescence from nonrelaxed excited-state conformations and thus blue-shifted and broadened. Experiments show indeed that, on the average, compounds having longer characteristic fluorescence times tend to exhibit larger Stokes shifts. When such fast reactions are studied as in the present case, the dynamical behavior of solvent molecules, that is, the time necessary to adopt the optimal coordination geometry for the excited state, should also play a relevant role. Our calculations show indeed that the energetic cost of imposing to S_1 the solvent coordination optimized for S_0 is ca. 1000 cm^{-1} , and this value could change for different derivatives having different first solvation shells.

4.3 Time-Resolved Fluorescence. 4.3.a. Experimental Fluorescence Decays. Fluorescence decays were recorded for $\sim 2.5 \times 10^{-3} \text{ mol/dm}^{-3}$ aqueous solutions at 330 nm after 267 nm excitation. Total fluorescence intensities were constructed from parallel and perpendicular excitation as described above. The resulting decay curves for uracil, 6-methyluracil, 1,3-dimethyluracil, 5-methyluracil (thymine), and 5-fluorouracil are shown in Figure 6. (Fluorescence decays of all uracils are given in the Supporting Information.)

Also displayed in this figure is the 330 fs (fwhm) Gaussian apparatus function. As can be seen, the fluorescence decays of the first three compounds are extremely fast, barely longer than the apparatus function. The fluorescence decays of two 5-substituted compounds, on the other hand, are much longer.

A thorough comparative analysis of the fluorescence decays of the 11 derivatives reveals that uracil, 1-methyluracil, 3-methyluracil, 6-methyluracil, and 1,3-dimethyluracil possess very rapid decays. A monoexponential model was used for the parameter estimation, and the fluorescence lifetimes were found to be about 100 fs (Table 4). This may be limited by the apparatus function of the upconversion system. The initial fluorescence anisotropies (r_0) were found to be close to 0.4 (which is the upper limit for parallel absorption and emission transition dipoles). The fluorescence is too short-lived to really

(88) Brady, B. B.; Peteanu, L. A.; Levy, D. H. *Chem. Phys. Lett.* **1988**, *147*, 538–543.

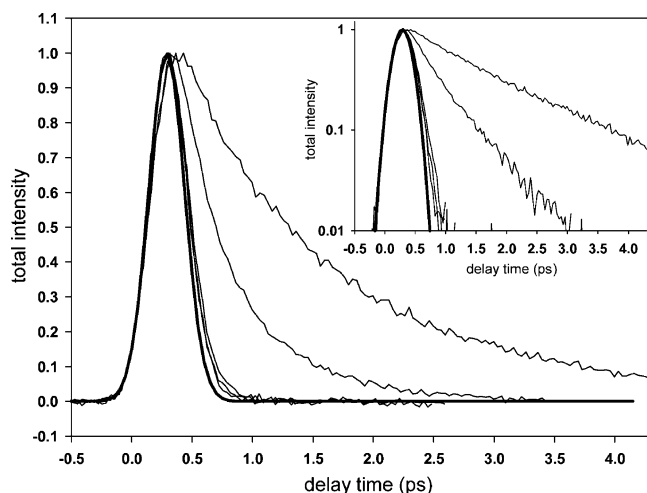


Figure 6. Fluorescence decays at 330 nm after excitation at 267 nm of five uracils in room-temperature aqueous solutions ($\sim 2.5 \times 10^{-3}$ mol/dm³): (in increasing order) uracil, 6-methyluracil, 1,3-dimethyluracil, 5-methyluracil (thymine), and 5-fluorouracil. Also shown is the 330 fs (fwhm) Gaussian apparatus function. The insert shows the same curves on a semilog scale.

characterize the decay of the fluorescence anisotropy, but interestingly, this seems to decay faster than the 10–20 ps expected from rotational diffusion.⁵

It can be seen that the only position that affects significantly the excited-state lifetime is C5. A biexponential model was used for the parameter estimation, and the fluorescence lifetimes were found to contain one ultrafast component varying between 100 and 700 fs and one much slower component (Table 4). With increasing lifetime the order is



Notably, the fluorescence of thymine and 1-methylthymine, which are methylated on the 5 position, decays about 4 times slower than the fluorescence of uracil and the 1-, 3-, and 6-methylated derivatives. In particular, 5-fluorination makes the excited-state lifetime substantially longer, for both uracil and 1,3DMU. Interestingly, the lifetime of 5F1,3DMU is shorter than that for 5FU. A slight decrease of the initial anisotropy was also observed for the thymines (5-methylated uracils).

No general correlation between the fluorescence lifetimes and any other observable can be established, but for the compounds displaying biexponential decays, there is a strong correspondence between the slow component, ranging from 0.3 and 1.8 ps and the lifetimes calculated by eq 5, the latter ones being slightly longer (about 0.2 ps).

4.3.b. Computed S_0 – S_1 Conical Intersection. To understand how the nature of the substituents affect the fluorescence lifetime, we have located the S_1/S_0 conical intersection (CI) at the CASSCF 8/8 level for three representative compounds, namely, uracil, thymine, and 5-fluorouracil. Confirming previous computational results on uracil,³¹ one of the key motions to reach the S_1/S_0 conical intersection is the pyramidalization at C5 (Figure 7), while an out of plane motion of the H5 hydrogen atom (or of the C5 substituent) leads the C5 substituent toward a “pseudo perpendicular” arrangement with respect the molecular plane (Figure 5).

With the aim of exploring more thoroughly the excited-state PES in the region connecting the FC to the CI, we then

computed some bidimensional (2D) maps of the S_1 surface at the PCM/TD-PBE0/6-31G(d) level. To build each map, we consider the structures of the minimum of the S_1 state (Min- S_1) and of the conical intersection (CI) and explore the part of the S_1 surface which connects them.

Restricting the 3N-6 dimensional space to a 2D one is clearly arbitrary, and a purposely tailored study of the vibrational modes connecting the FC region to the CI should be necessary in order to unambiguously assess the dynamical motion on the S_1 PES. As a first step in this direction, on the basis of our computational results, we choose to focus on the out of plane motion of the C5 substituent (ϕ improper dihedral). The second “collective” coordinate x (giving account also for the C5 pyramidalization) is instead defined imposing that all the other internal coordinates move in a synchronous way, as specified in the section of computational methods. Inspection of Figure 7 (additional figures are shown in the Supporting Information) supports the reliability of the conical intersection structure located at the CASSCF level. In the region of the configurations space close to the CI point, the S_0 and the S_1 PESs are extremely close (energy difference ≤ 0.2 eV ($\leq 1.6 \times 10^3$ cm⁻¹)) both in the gas phase and in aqueous solution. Also, when the effect of dynamical correlation is included by TD-DFT and solvent effect by the PCM method, it is thus confirmed that the conical intersection is reached by out of plane motion of the C5 substituent. For uracil, the S_1 PES in the region connecting Min- S_1 and CI (Figure 8) is flat, and the height of the energy barrier separating Min- S_1 and CI is small (~ 0.1 eV, $\sim 8 \times 10^2$ cm⁻¹), in line with the very small fluorescence lifetime (see below).

The results obtained for thymine and 5-fluorouracil are similar, but the height of the barrier between Min- S_1 and CI is larger than in uracil. Its value can be estimated to ~ 0.2 eV ($\sim 1.6 \times 10^3$ cm⁻¹) for thymine and in the range 0.5–1 eV ($(4-8) \times 10^3$ cm⁻¹) for 5-fluorouracil. These results show that, for thymine and, even more, for 5-fluorouracil, the out of plane motion is more difficult than for uracil. The above values should be considered as only qualitative estimates. They have not been obtained by a real minimum energy path leading from Min- S_1 and CI. Furthermore, from the computational point of view, even if our TD-DFT results are in good agreement with experiments, more accurate electronic structure calculations should probably be necessary to describe the behavior of the excited state in the proximity of the conical intersection. Notwithstanding those limitations, it is important to highlight that the relative ordering of the barrier height is in line with the excited-state lifetimes, supporting our explanation of the fluorescence lifetime experiments.

5. Discussion

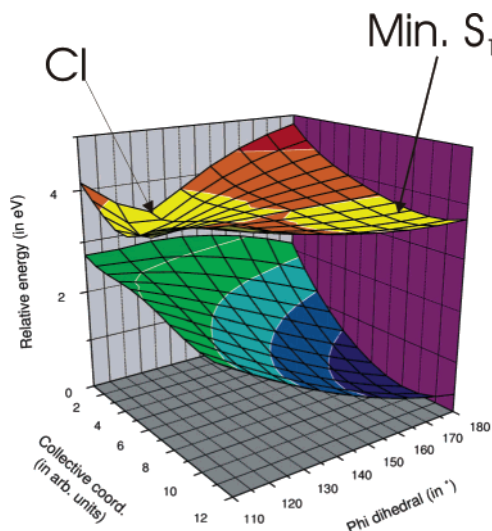
The experimental and computational results hereby presented provide a similar and consistent picture of the photophysical behavior of uracil-like molecules in aqueous solution.

First, according to both experiments and calculations, the relevant transition for discussing the absorption and fluorescence spectra of uracil derivatives in aqueous solution should be the π/π^* transition. This is corroborated by the facts that the anisotropy is close to 0.4, the computations show that this state always corresponds to the S_1 state, and that the dependence of the excited-state lifetime on the C5 position can be easily explained on the weight of this atom in the HOMO. On the

Table 4. Measured Characteristic Times (fs) of the Fluorescence Decays of Uracil and Its Derivatives.^a Also Given are the Radiative Lifetimes as Calculated by the Strickler–Berg Relation and the Corresponding Fluorescence Lifetimes as Calculated by Equation 5

compound	α	τ_1 (fs)	τ_2 (fs)	$\langle\tau\rangle$ (fs)	$\tau_{\text{rad,SB}}$ (ns)	$\tau_{1,\text{SB}}$ (ps)
U	1	96 ± 3			7.01	0.25
1MU	1	93 ± 4			7.25	0.35
3MU	1	92 ± 4			9.06	0.35
6MU	1	97 ± 3			7.35	0.45
T	0.56 ± 0.02	195 ± 17	633 ± 18	388 ± 13	7.72	0.78
1,3DMU	1	118 ± 3			7.54	0.35
1MT	0.62 ± 0.01	192 ± 12	721 ± 16	392 ± 10	7.45	1.02
5FU	0.39 ± 0.04	694 ± 56	1736 ± 53	1325 ± 49	10.12	2.24
5CIU	0.68 ± 0.01	155 ± 10	539 ± 15	279 ± 9	9.23	0.84
TFT	0.88 ± 0.11	142 ± 2	328 ± 9	165 ± 3	8.11	0.52
5F1,3DMU	0.43 ± 0.01	246 ± 20	1075 ± 17	717 ± 13	8.74	1.75

^a Also given are the uncertainties from the fit (one standard deviation), not to be confused with the experimental uncertainty of 100 fs.

**Figure 7.** S_0 and S_1 potential energy surfaces (in eV) in the region connecting the minimum of the π/π^* state and the S_0/S_1 conical intersection for uracil.

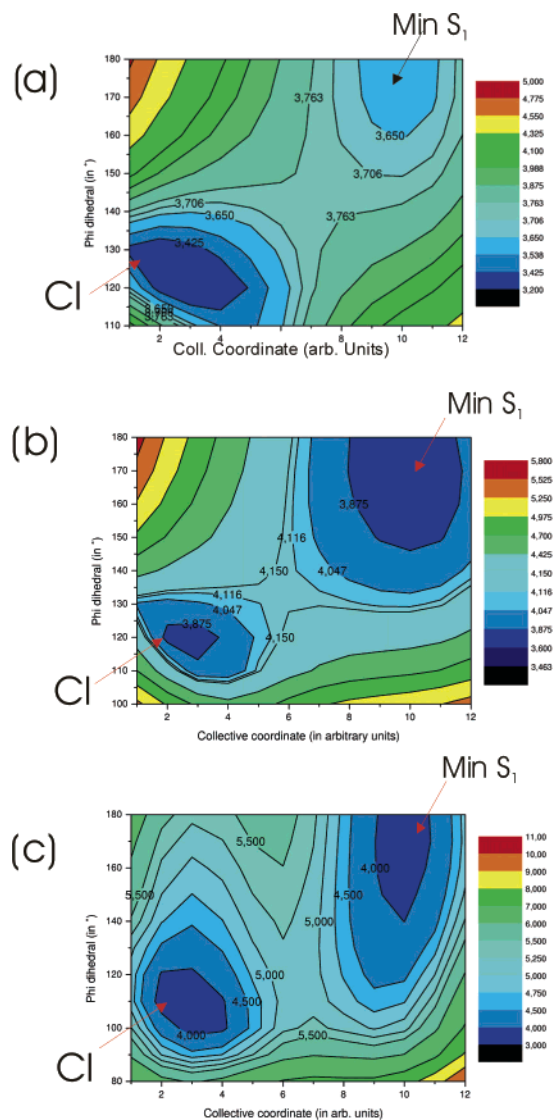
other hand, the involvement of the n/π^* excited state would probably be related to a pyramidalization of the carbonyl carbon atom, and thus it would be less sensitive to the nature of the C5 substituent. As a consequence, the involvement of the n/π^* state that has been sometimes invoked in the literature to explain the low fluorescence quantum yield⁸⁹ should be ruled out.

Obviously, the above considerations hold only in aqueous solution: the involvement of the n/π^* state is extremely likely in the gas phase or in apolar solvents. Indeed, our calculations show that in vacuo the lowest energy transition always corresponds to the n/π^* excitation HOMO-1/LUMO (Figure 3). This indication is in line with the experimental results on thymine, showing that, following S_2/S_1 decay, the system is trapped in a dark state.^{39–41}

Experiments and calculations agree in predicting that excitation on the π/π^* state leads to significant geometry distortion, consistent with a Stokes shift of ~ 1 eV ($\sim 8 \times 10^3$ cm^{-1}). Excited-state geometry optimization in aqueous solution shows indeed the existence of an energy minimum for the π/π^* state that, besides the variations in the C4C5 and C5C6 bond lengths, is characterized by a nonplanar, boat-like structure.

It is interesting to note that CASSCF calculations³¹ in the gas phase fail to locate a true minimum on the π/π^* surface. Indeed, a planar minimum, found only within C_s symmetry,

(89) Turpin, P. Y.; Peticolas, W. L. *J. Phys. Chem.* **1985**, *89*, 5156–5160.

**Figure 8.** S_1 potential energy surfaces (in eV) connecting the minimum of the π/π^* state and the S_0/S_1 conical intersection: (a) uracil; (b) thymine; (c) 5-fluorouracil. PCM/TD-PBE0/6-31G(d) calculations in aqueous solution.

reveals itself as a saddle point when relaxing the planarity constraint, and out of plane motion leads to a conical intersection with the more stable n/π^* state. Our preliminary TD-DFT calculations in the gas phase provide similar indications, showing that distortion from the planarity leads to significant mixing between the two lowest energy electronic states, and that the n/π^* state is always more stable than the π/π^* state.

This result strongly suggests that the existence of a minimum on the π/π^* surface is due to solvent effect, significantly stabilizing the π/π^* over the n/π^* state.

For what concerns the excited state decay, our results indicate that also in aqueous solution the key step consists of the pyramidalization of the C5 carbon atom and in the out of the plane motion of the C5 substituent. Not only the calculations show that a representative set of the compounds examined undergoes the above geometrical rearrangements in the conical intersection, but the comparison of the experimental excited-state lifetime shows that the only critical position is C5.

Pyramidalization at carbon atoms is frequently involved in CI, in molecules with π aromatic systems, involving an excited state deriving from a π/π^* electronic excitation, since a distortion of the π electron system obviously affects the ground state more than the excited state.^{90–95} According to those considerations, it can be explained why pyramidalization involves the C5 carbon atom more than the C6. The C5 carbon atom contributes more than C6 to the π HOMO of uracil-like molecules, and this orbital is bonding between C5 and C4 and antibonding between C6 and N1. In uracil derivatives, pyramidalization at the C5 and out of plane motion of C5 substituents is expected to destabilize the ground state more than at C6. Consequently, it should be expected that the ability of substituents to stabilize C5C6 and C4C5 π bonding modulates the energy barrier toward the conical intersection, influencing the excited-state lifetime. Electron donor and/or hyperconjugative substituent on C5 increases the energy required to reach the CI from Min- S_1 , explaining why the excited-state lifetimes for 5-fluorouracil, 5-chlorouracil, and thymine are significantly longer than that of uracil. On the other hand, both inductive and hyperconjugative effects due to the strongly electronegative trifluoromethyl substituent are less significant than for methyl, explaining why the excited-state lifetime of trifluorothymine is shorter than that of thymine.

The PES associated with the path leading from Min- S_1 to CI is consistent with a very fast excited-state decay. It is indeed significant that the Min- S_1 is already more stable than the Franck–Condon point by ~ 1 eV ($\sim 8 \times 10^3$ cm⁻¹). Once Min- S_1 is reached, the kinetic energy of the wave packet should be enough to easily overcome the small energy barrier toward the CI since it also has the right inertia toward the out of plane motion.

The above considerations, though providing a consistent explanation for the observed excited-state lifetime trend, can be considered at the moment only qualitative. First, the excited-state lifetime is probably modulated not only by the electronic effects discussed above but also by dynamical factors related to the different weight of the substituents. This latter kind of effects could explain, for example, why the excited-state lifetime of trifluorothymine is longer than that of uracil, although the electronic barrier for C5 pyramidalization of those two com-

pounds should be similar. Furthermore, a detailed fully dynamical study, probably involving more than two coordinates, with a careful analysis of the excited state surface would be necessary to unambiguously assess the behavior of a wave packet on S_1 .

Recent studies have indeed shown that effects, such as the exact curvature of the PES (for example, the presence of wide plateau)^{96,97} or the existence of large conical intersection seam,⁹⁸ remarkably influence the excited-state dynamics of several systems. The interaction between different electronic states, coupled by vibronic interaction (for example, by the out of plane motion of the carbonyl group) or by the solvent molecules motion (vide infra), could also play some role. Finally, recent calculations have suggested the involvement of triplet–singlet intersystem crossing in the cytosine excited-state decay.¹⁷ All of these effects could be, in principle, involved in the uracil derivatives' excited-state dynamics, giving account (for example, ref 96) of the biexponential behavior found in some of the compounds under study.^{4–7}

On the other hand, notwithstanding the above limitations, the picture of the uracil derivatives behavior we provided can be considered a good starting point for future work and can be fruitfully compared with results relative to the other nucleobases. Even if several important features are not completely understood, the very fast excited-state decays of uracil (see also ref 31), thymine, cytosine,^{8,9} adenine,¹² and guanine–cytosine pair¹⁴ share some common features. In all these compounds, a very low barrier (~ 0.1 eV, $\sim 8 \times 10^2$ cm⁻¹) should separate the minimum of the bright state from an easily accessible S_1/S_0 conical intersection. Out of plane deformation of a carbon atom in a six-membered ring (with a “perpendicular arrangement” of one of the substituents) should be the crucial mechanistic step toward the conical intersection region. Within this general mechanism, due to the different shape of the orbitals involved in the S_0 – S_1 transition, the nature of the atom undergoing to pyramidalization changes: C5 in thymine and uracil, C6 in cytosine,^{8,9} and C2 or C6 in adenine.¹²

In all of the above compounds a low-lying n/π^* dark state can be involved in the excited-state dynamics, leading to long-lived excited states.^{39–41} However, its role should be more relevant in the gas phase or in apolar solvent, due to the destabilization of the n/π^* state and the stabilization of the π/π^* state in polar solution. This has been suggested in the case of adenine,¹² and the present results show that this is true for uracil and thymine. Indeed, it is worth noting that there are several experimental results indicating that excited-state lifetimes of uracil, thymine, and adenine are shorter in water solution than in the gas phase.²

Those latter considerations highlight the importance of a reliable treatment of solvent effect. We have shown that only taking into account both bulk effects and explicit solvent molecules it is possible to reproduce solvent effects on the energy and the intensities of the absorption and fluorescence spectra. Obviously, when studying extremely fast reactions in aqueous solution, the dynamical role of solvent molecules could be relevant. As a matter of fact, the evolution of uracil's excited state strongly depends on the behavior of π and π^* orbitals, whose relative energy could be significantly influenced by the

- (90) Bernardi, F.; Olivucci, M.; Robb, M. A. *Chem. Soc. Rev.* **1996**, 321.
(91) Klessinger, M.; Michl, J. *Excited states and photochemistry of organic molecules*; VCH: New York, 1999.
(92) Domcke, W.; Yarkony, D. R.; Köppel, H., Eds. *Conical intersections: electronic structure, dynamics and spectroscopy*; World Scientific: New Jersey, 2004; Vol. 15.
(93) Ben-Nun, M.; Quenneville, J.; Martínez, T. J. *J. Phys. Chem. A* **2000**, *104*, 5161–5175.
(94) Leitner, D. M.; Levine, B.; Quenneville, J.; Martínez, T. J.; Wolynes, P. G. *J. Phys. Chem. A* **2003**, *107*, 10706–10716.
(95) Quenneville, J.; Martínez, T. J. *J. Phys. Chem. A* **2003**, *107*, 829–837.

- (96) Olivucci, M.; Lami, A.; Santoro, F. *Angew. Chem., Int. Ed.* **2005**, *117*, 5248–5251.
(97) Improta, R.; Santoro, F. *J. Chem. Theory Comput.* **2005**, *1*, 215–229.
(98) Hunt, P. A.; Robb, M. A. *J. Am. Chem. Soc.* **2005**, *127*, 5720–5726.

formation of short-lived adducts with perpendicularly bound solvent molecules. Moreover, the solvation shells of the ground, n/π^* , and π/π^* states are very different, suggesting that their relative energy or their coupling could change following the motion of just a single solvent molecule.³² Only a dynamical treatment, including a larger number of explicit solvent molecules, could provide a definite answer to the above questions.

On the other hand, it is important to highlight that, to the best of our knowledge, this is the first time that solvent is included in a meaningful way in the study of fluorescence spectra, as shown by the good agreement with the experimental results for what concerns both absorption and emission spectra. This is a very encouraging result for what concerns the possibility of a complementary experimental and computational approach. It is not easy, indeed, to directly use the results of gas-phase calculations to explain the behavior in the condensed phase (mostly in aqueous solution).

6. Conclusions

In this paper, a complete picture of the excited-state behavior of uracils is given, by analyzing in detail, both experimentally and by means of quantum chemical calculations, the absorption and emission spectra of 11 derivatives of uracil and by determining their excited-state lifetimes.

The absorption spectra are mainly determined by the nature of the substituent of the N1 nitrogen and C5 carbon atoms. Electron donor and/or hyperconjugative substituents in those positions lead to a red shift of absorption peak (corresponding to the HOMO–LUMO π/π^* transition) with respect to that of uracil, while their effect is opposite in position 6. PCM/TD–DFT calculations in aqueous solution provide similar indications and allow for a rationalization of this behavior based on the shape of the HOMO–LUMO orbitals.

All of the compounds examined exhibit large Stokes shifts (~ 1 eV, $\sim 8 \times 10^3$ cm⁻¹), suggesting a remarkable geometry rearrangement on the excited state. TD–DFT geometry optimizations in aqueous solution confirm the above picture, showing that, besides the changes in the interatomic bond distances, on the minimum on the S_1 surface, the pyrimidine ring significantly deviates from the planarity, adopting a boat-like structure. The good agreement between the computed and the experimental fluorescence maxima not only supports the reliability of our computational approach, but it confirms that the emission occurs from the π/π^* bright state.

Experiments show that the excited-state lifetime of all the compounds examined, except 5-fluorouracil, is dominated by a component shorter than 250 fs. Calculations help to rationalize the above finding, showing that a small energy barrier separates the minimum on the S_1 surface from the S_0/S_1 conical intersection, characterized by pyramidalization and out of plane motion of the substituents on the C5 atom. The energetic cost for that rearrangement is modulated by the chemical nature (due to inductive or hyperconjugative effect) of the C5 substituent. Our calculations show indeed that reaching the CI is more difficult for thymine, and even more so for 5-fluorouracil, than for uracil, giving account of the ordering of the excited-state lifetime.

Finally, from the methodological point of view, the very recent availability of analytical TD–DFT gradient, including solvent effects by means of PCM, allows for the first time the accurate computation of fluorescence spectra, increasing the possibility of complementing computational and experimental results in the condensed phase. Due to the complexity of the excited-state processes of the nucleobases in protic solution, the indications provided by integrated experimental/computational approaches can be extremely useful for reaching a full understanding of their photophysical behavior.

Acknowledgment. The authors thank the European CERC3 (Chairmen of the European Research Councils) program “Photochemistry of Nucleic Acids” and MIUR for financial support. The stay of Á.B. was made possible by a Marie Curie Host Fellowships from the European Commission (Contract Number HPMT-CT-2001-00357). R.I. thanks Dr. Fabrizio Santoro for help in building the two-dimensional surfaces and useful discussions. All the calculations have been performed using the advanced computing facilities of the “Campus Grid”, University Federico II, Naples.

Supporting Information Available: Notes regarding the choice of PBE0 functional, log-normal functions, fluorescence quantum yield measurements, geometries for conical intersections obtained from quantum chemical calculations, additional figures illustrating steady-state absorption and fluorescence spectra, as well as fluorescence decays curves. This material is available free of charge via the Internet at <http://pubs.acs.org>.

JA056181S